

Preparation and Properties of the System Cu_xPd_{1-x}O (0 ≤ x ≤ 0.175)

C-M. NIU, P. H. RIEGER, K. DWIGHT, AND A. WOLD*

*Department of Chemistry, Brown University, Providence,
Rhode Island 02912*

Received November 27, 1989; in revised form February 15, 1990

Samples of Cu_xPd_{1-x}O were prepared by codecomposition of the nitrates. Single-phase products were obtained for $x \leq 0.15$. The presence of Cu(II) in D_{2h} symmetry coordination has been confirmed by magnetic susceptibility and ESR spectra. The results are discussed, compared with those of the system Cu_xMg_{1-x}O, and interpreted in terms of the Cu(II) coordination symmetry and the electron orbitals. © 1990 Academic Press, Inc.

Introduction

The structure of copper(II) oxide contains Cu(II) with essentially square planar coordination of oxygen around copper (1). This coordination is also found to exist in the high T_c superconducting oxides (2, 3). The structure of copper(II) oxide is shown in Fig. 1, and the essentially square planar coordination of the oxygen around the copper is clearly seen. The space group is $C2/c$ with unit cell dimensions $a = 4.6837(5) \text{ \AA}$, $b = 3.4226(5) \text{ \AA}$, $c = 5.1288(6) \text{ \AA}$, and $\beta = 99.54(1)^\circ$. The structure is a distorted PdO type, and each copper has four O' neighbors at 1.96 Å and two apical oxygens, O'' at 2.78 Å.

The magnetic susceptibility of copper(II) oxide shows an anomaly at 230 K which has been interpreted as an indication for anti-ferromagnetic ordering (4, 5). This was confirmed by neutron diffraction (6), though subsequent neutron diffraction studies of single crystals have indicated the

presence of an additional spin reordering transition at 215 K (7, 8). No ESR spectrum has been observed for the square planar copper(II) in copper(II) oxide because there is sufficient electron delocalization to obscure the ESR spectrum (9).

The structure of PdO was reported by Huggins as well as Moore and Pauling and was confirmed by Waser (10-12). The compound crystallizes with space group $P4_2/mmc$ with two PdO molecules per unit cell. The cell parameters are $a = 3.03(1) \text{ \AA}$ and $c = 5.33(1) \text{ \AA}$. The atomic positions are: two Pd at (0 0 0), $(\frac{1}{2} \frac{1}{2} \frac{1}{2})$ and two O at $(\frac{1}{2} 0 \frac{1}{4})$, $(\frac{1}{2} 0 \frac{3}{4})$. The structure of PdO is shown in Fig. 2. Each oxygen atom is bound to four palladium atoms at the corners of a nearly regular tetrahedron, and each palladium atom forms four coplanar bonds to oxygen atoms at the corners of the rectangle. The structure of copper(II) oxide can be seen as a distorted PdO type. There are no reports in the literature concerning the extent of solid solution between CuO and PdO. It was thought that PdO might be an excellent host for investigation of square planar-coordi-

* To whom all correspondence should be addressed.

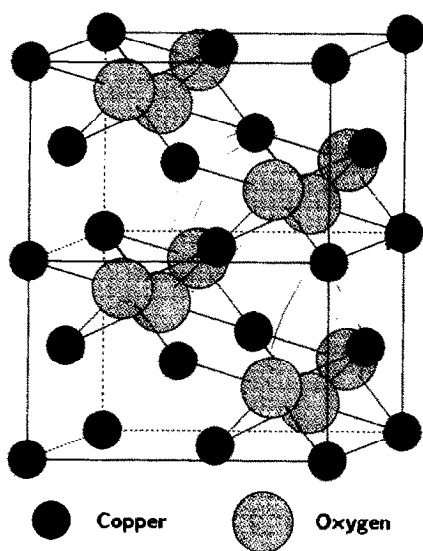


FIG. 1. Structure of copper(II) oxide.

nated Cu(II) both as to its magnetic properties and electron spin resonance. The possibility of obtaining localized square planar Cu(II) in a PdO matrix resulted in this study of the system $\text{Cu}_x\text{Pd}_{1-x}\text{O}$.

Experimental

Samples of $\text{Cu}_x\text{Pd}_{1-x}\text{O}$ were prepared by codecomposition of the corresponding nitrates. The starting materials were high purity copper metal (5–9's, Aesar Chemical Co.) and palladium metal (3–9's, Strem Chemical, Inc.). Both copper and palladium metal were prereduced in 85%Ar/15% H_2 at 450 and 900°C, respectively. The palladium was then heated under vacuum at 350°C for $\frac{1}{2}$ hr to drive off the adsorbed H_2 . The appropriate weights of copper and palladium metals were dissolved in 1:1 nitric acid in order to convert the metals to the corresponding nitrates. The solution was dried on a hot plate and then decomposed at 350°C for 6 hrs, ground, and heated at 500°C for 36 hr. During the heating period,

the samples were cooled to room temperature and ground twice.

X-ray diffraction patterns of samples were obtained with a Philips–Norelco diffractometer using monochromatic high intensity $\text{CuK}\alpha_1$ radiation ($\lambda = 1.5405 \text{ \AA}$). For the qualitative identification of the phase present, the diffraction patterns were taken from $12^\circ < 2\theta < 72^\circ$ with a scan rate of $1^\circ 2\theta/\text{min}$ and a chart speed of 30 in./hr. The scan rate used to obtain X-ray patterns for precision cell constant determination was $0.25^\circ 2\theta/\text{min}$ with a chart speed of 30 in./hr. The cell parameters were determined by a least-squares refinement of the reflections, using a computer program which corrects for the systematic errors of the measurement (13).

Magnetic susceptibility measurements over the temperature range 77–530 K were carried out using a Faraday balance with a field strength of 10.4 kOe. Field dependency measurements were carried out at both 77 K and room temperature. Electron spin resonance spectra were recorded using a Bruker ER220D spectrometer.

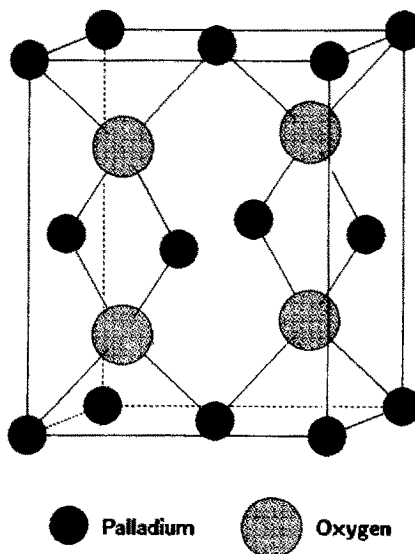


FIG. 2. Structure of palladium oxide.

Results and Discussion

Samples of the copper-palladium oxide system $\text{Cu}_x\text{Pd}_{1-x}\text{O}$ were prepared by the co-decomposition of copper and palladium mixed nitrates. Attempts to substitute 2.0 mol% of palladium for copper in copper(II) oxide gave an X-ray diffraction pattern of the product which showed the presence of unreacted PdO. Hence, there does not appear to be any appreciable solubility of palladium in copper(II) oxide. From X-ray diffraction analysis it was observed that samples containing up to 15 mol% of copper in PdO were single-phase materials. For the sample containing 17.5 mol% copper, step counting over the (111) reflection of CuO at a 2θ angle of 38.74° indicated the presence of a separate copper(II)-phase oxide. The structure of PdO is shown in Fig. 2 and the system $\text{Cu}_x\text{Pd}_{1-x}\text{O}$ ($0 \leq x \leq 0.15$) crystallizes with this structure. The cell parameters are given in Table I and it can be seen that there is a slight decrease in both a and c parameters as copper(II) is substituted for palladium(II).

Magnetic susceptibility measurements

TABLE I
PROPERTIES OF POLYCRYSTALLINE $\text{Cu}_x\text{Pd}_{1-x}\text{O}$

x	Cell parameters (\AA)			Weiss constant (K)	
	a	c	$\mu(\text{BM})$		
0.00	3.044(2)	5.328(5)	—	—	
0.05	3.036(2)	5.331(5)	1.85	-70	
0.10	3.032(2)	5.327(5)	1.83	-129	
0.15	3.029(2)	5.307(5)	1.81	-217	

were made as functions of both applied field and temperature. The magnetic susceptibility data are plotted in Fig. 3 as reciprocal susceptibility versus temperature. All of the copper-containing samples showed paramagnetic behavior, and the results are tabulated in Table I. No field dependency was observed, but it can be seen from the Weiss constants in Table I that antiferromagnetic interactions are present. The effective moments given in Table I compare favorably with the spin-only value of 1.73 BM. However, the Weiss constants are seen to increase, which is consistent with the increase in the copper content. In a pre-

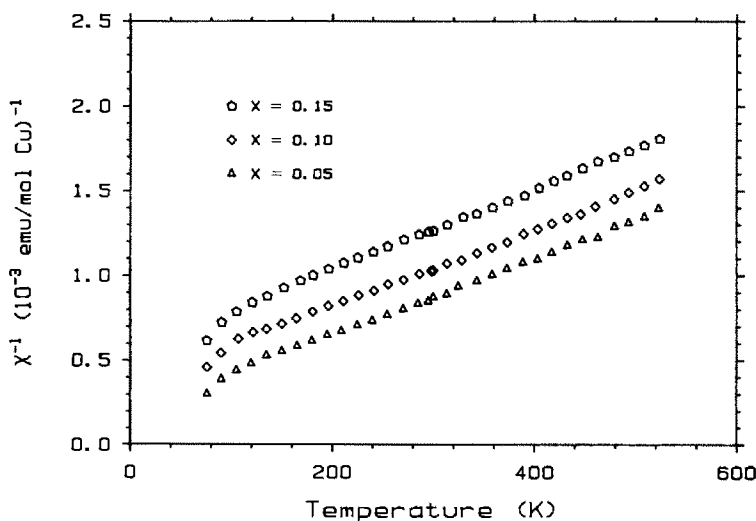


FIG. 3. Temperature dependence of the inverse magnetic susceptibility of members of the system $\text{Cu}_x\text{Pd}_{1-x}\text{O}$.

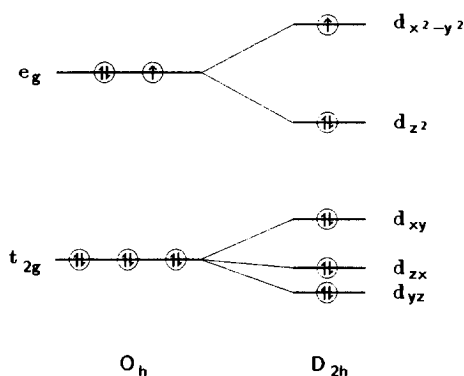


FIG. 4. Electron energy levels of the Cu(II) in octahedral (O_h) and square planar (D_{2h}) symmetries.

vious study of the system $Cu_xMg_{1-x}O$ (14), samples containing up to 15 mol% of copper showed almost ideal Curie behavior. A partial explanation of the observed difference in the magnetic behavior of copper(II) in MgO and PdO can be related to a difference in the copper symmetry. In the PdO structure, Cu(II) assumes a distorted square planar (D_{2h}) symmetry, whereas in MgO, Cu(II) is octahedrally coordinated (O_h). Figure 4 compares the one-electron energy diagrams of copper(II) in both crystallographic environments. It can be seen that for the substitution of Cu(II) for magnesium in an octahedral site, the e_g orbitals are degenerate and are $\frac{3}{4}$ filled, whereas in a square planar environment, the degeneracy is removed and the $d_{(x^2-y^2)}$ orbital is half-filled. Thus according to the rules of superexchange, the antiferromagnetic coupling of the unpaired electron in the half-filled $d_{(x^2-y^2)}$ orbital via oxygen p -orbitals in the $Cu_xPd_{1-x}O$ structure is stronger than the interactions present in the $Cu_xMg_{1-x}O$ system. A further consideration which undoubtedly plays a role in the differences observed in the magnetic properties of $Cu_xPd_{1-x}O$ and $Cu_xMg_{1-x}O$ is the electronic behavior of the host structure. MgO is an insulator whereas PdO shows

$g_x = 2.077$	$ A_x = (22.9 \pm 0.8) \times 10^{-4} \text{ cm}^{-1}$
$g_y = 2.066$	$ A_y = (10.3 \pm 1.0) \times 10^{-4} \text{ cm}^{-1}$
$g_z = 2.334$	$ A_z = (154.3 \pm 0.3) \times 10^{-4} \text{ cm}^{-1}$

metallic behavior which may affect the nature of the superexchange interactions.

ESR spectra were obtained of CuO/PdO samples, ranging in CuO content from 15 to 0.2%. Although the overall shape of the spectrum was independent of copper concentration, the resolution improved dramatically as the concentration decreased. The most dilute sample gave the spectrum shown in Fig. 5 where the $m_{Cu} = \pm \frac{3}{2}$ parallel features are well resolved into ^{63}Cu and ^{65}Cu contributions. The g -tensor and ^{63}Cu hyperfine tensor components were determined by a nonlinear least-squares fitting procedure (15) and are given in Table II.

The g -tensor anisotropy is due to spin-orbit admixture of d_{yz} , d_{zx} , and d_{xy} character into the predominantly $d_{(x^2-y^2)}$ copper orbital containing the unpaired electron; these admixtures contribute to g_x , g_y , and g_z , respectively. The departure from axial

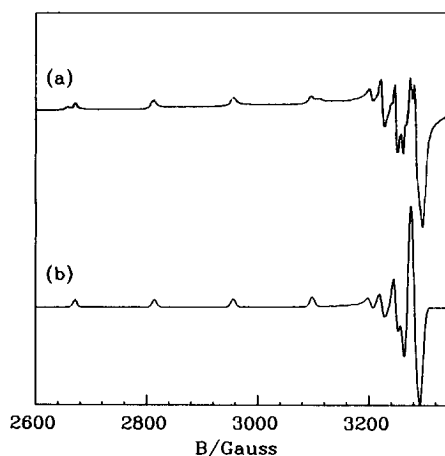


FIG. 5. (a) ESR spectrum of 0.2% CuO in PdO at 150 K $V_0 = 9.461$ GHz; (b) computer-simulated spectrum using parameters of Table II.

symmetry thus reflects lifting of the degeneracy of the d_{zx} and d_{yz} orbitals. If A_x and A_y have the same sign, spin-orbit coupling effects almost entirely account for the departure of the hyperfine tensor from axial symmetry. If A_x and A_y have different signs, we would have to invoke admixture of up to 0.4% d_{z^2} character to account for the hyperfine tensor. Using equations given by McGarvey (16, 17) and the dipolar coupling parameter, $P = 0.0399 \text{ cm}^{-1}$ (18), we can estimate the metal $d_{(x^2-y^2)}$ contribution to the orbital containing the unpaired electron, $\rho_d = 0.76\text{--}0.86$, depending on the signs of the perpendicular hyperfine components; the remaining spin density is presumably in metal 4s and 4p and oxygen contributions to the half-occupied orbital.

The ESR spectrum of CuO in PdO is dramatically different from that in MgO, where the spectrum is isotropic at 77 K with $\langle g \rangle = 2.192$, $\langle A^{\text{Cu}} \rangle = 18.6 \times 10^{-4} \text{ cm}^{-1}$ (19). Line-width effects in the 77 K spectrum suggested a process which averages the g - and hyperfine tensor anisotropies. Coffman (20) found that an anisotropic spectrum is obtained at liquid helium temperatures, but one very different from that expected for Cu(II) if the tetragonal distortion is static; his results could be explained assuming quantum mechanical tunneling between equivalent tetragonal distortions of the octahedral Cu^{2+} site. Using Coffman's results and the above value of P , we can estimate $\rho_d = 0.64$. Thus, quite apart from the dynamical Jahn-Teller distortions in MgO, the copper d -electron spin density is significantly lower in MgO than in PdO, suggesting greater delocalization of spin in MgO. This result is consistent with the interpretation of the magnetic susceptibility data if we distinguish between spin delocalization into oxygen orbitals (greater in the $\text{Cu}_x\text{Mg}_{1-x}\text{O}$ system) and spin polarization of oxygen orbitals (greater in the $\text{Cu}_x\text{Pd}_{1-x}\text{O}$ system).

Acknowledgments

The research received partial support from the National Science Foundation, DMR 880 3184, the Office of Naval Research, Eastman Kodak Co., and the Exxon Education Foundation.

References

1. J. M. LONGO AND P. M. RACCAH, *J. Solid State Chem* **6**, 526 (1973).
2. D. W. MURPHY, S. SUNSHINE, R. B. VAN DOVER, R. J. CAVA, B. BATLOGG, S. M. ZAHURAK, AND L. F. SCHNEEMEYER, *Phys. Rev. Lett.* **58**, 1888 (1987).
3. M. A. SUBRAMANIAN, C. C. TORARDI, J. C. CALABRESE, J. GOPLAKASHNAN, K. J. MORRISSEY, J. R. ASKEY, R. B. FLIPPEN, U. CHOWDY, AND A. W. SLEIGHT, *Science* **239**, 1015 (1988).
4. M. O'KEEFE AND F.S. STONE, *J. Phys. Chem. Solids* **23**, 261 (1962).
5. B. RODEN, E. BRAUN, AND A. FREIMUTH, *Solid State Commun.* **64**, 1051 (1987).
6. B. X. YANG, J. M. TRANQUADA, AND G. SHIRANE, *Phys. Rev. B* **38**, 179 (1988).
7. J. B. FORSYTH, P. J. BROWN, AND B. M. WANKLIN, *J. Phys. C* **21**, 2917 (1988).
8. B. X. YANG, T. R. THURSTON, J. M. TRANQUADA, AND G. SHIRANE, *Phys. Rev. B* **39**, 4343 (1989).
9. H. LUMBEEK AND J. VOITLÄNDER, *Z. Phys. Chem. (Frankfurt)* **79**, 225 (1972).
10. M. L. HUGGINS, *Chem. Rev.* **10**, 427 (1932).
11. W. J. MOORE AND L. PAULING, *J. Amer. Chem. Soc.* **63**, 1392 (1942).
12. JURG WASER, *Acta Crystallogr.* **6**, 661 (1953).
13. W. N. SCHREINER, C. SURDUKOWSKI, R. JENKINS, AND C. VILLAMIZER, *Norelco Rep.* **29**, 42 (1982).
14. X-M. LUO, P. WU, R. KERSHAW, K. DWIGHT, AND A. WOLD, *Mater. Res. Bull.* **23**, 1719 (1988).
15. J. A. DEGRAY AND P. H. RIEGER, *Bull. Magn. Reson.* **8**, 95 (1987).
16. B. R. MCGARVEY, in "Electron Spin Resonance of Metal Complexes" (T. F. Yen, Ed.), p. 1, Plenum, New York, 1969.
17. J. A. DEGRAY, Q. MENG, AND P. H. RIEGER, *Trans. Faraday Soc.* **1** **83**, 3565 (1987).
18. J. R. MORTON AND K. F. PRESTON, *J. Magn. Reson.* **30**, 582 (1978).
19. J. W. ORTON, P. AUZINS, J. H. E. GRIFFITHS, AND J. E. WERTZ, *Proc. Phys. Soc.* **78**, 554 (1961).
20. R. E. COFFMAN, *J. Chem. Phys.* **48**, 609 (1968).